PREPARATION OF
HYDROXYAPATITE POROUS SCAFFOLD

A THESIS SUBMITTED IN PARTIAL FULFILLMENT

OF THE REQUIREMENT FOR THE DEGREE OF

Bachelor of Technology

in

Ceramic Engineering

By

SIDDHARTHA BISWAL

(Roll No. 10608023)

Department of Ceramic Engineering

National Institute of Technology

Rourkela - 769008

CERTIFICATE

This is to certify that the thesis entitled, **"Preparation of Hydroxyapatite Porous Scaffold"** submitted by Mr. Siddhartha Biswal in partial fulfillment of the requirement for the award of Bachelor of Technology Degree in Ceramic Engineering at the National Institute of Technology, Rourkela (Deemed University) is an authentic work carried out by him under my supervision and guidance.

To the best of my knowledge, the matter embodied in the thesis has not been submitted in any other University/Institute for the award of any Degree or Diploma.

Date :

Prof. D. Sarkar

Dept. of Ceramic Engineering,

National Institute of Technology

Rourkela – 769008

ACKNOWLEDGEMENT

It is with happiness and endless gratitude that I am indebted to Prof. J. Bera, Head of the Department, Ceramic Engineering, National Institute of Technology, Rourkela for assigning me this project titled, “Preparation of Hydroxyapatite Porous Scaffold” and for all his invaluable inputs.

Prof. D. Sarkar, Associate Professor and my guide, has been a constant source of inspiration on both personal and project related issues. His suggestions and encouragements have always been present with the highest degree of honest inspiration.

I am highly grateful to Prof. S. Bhattacharya, Prof. S. Pratihar, Prof. S. Pal, Prof. R. Sarkar, Prof. R. Mazumder, Prof. A. Choudhary and Prof. B.B. Nayak for giving me their timely inputs and utmost guidance at all times.

This project wouldn’t have been highly successful without the appropriate help from Mr. S.K. Swain, Ph.D scholar in Ceramic Engineering Department of our institute. His smiling approach to each and every problem has carved out a special niche for itself.

This forum deserves a special mention to all the other Ph.D scholars, M.Tech scholars and lab assistants of the Departments of Ceramic Engineering, Metallurgical and Materials Science Engineering, Chemistry Science of our institute who have tirelessly extended their joyous support in all the labs whenever I needed them.

I thank the Library Department whole-heartedly for extending all sorts of help. Last but not the least, I thank all my friends who have been patient with all my endeavors all through the past and present year and beyond.

I salute you all.

Date : 04 May 2010

Siddhartha Biswal

Roll No. 10608023

B.Tech, Ceramic Engineering

N.I.T. Rourkela

CONTENTS

ABSTRACT

The present work deals with the preparation and study of bioceramic scaffold using hydroxyapatite powder as the source material. Hap powder was prepared by Co-Precipitation technique using $Ca(NO_3)_2.4H_2O$ and $(NH_4)_2HPO_4$ as raw materials. X-ray diffraction (XRD), Fourier Transform InfraRed (FTIR) spectroscopy and BET analysis were used to characterize the Hap powder and calculate its crystallite size, surface area and particle size. Polyethylene glycol (PEG – 600) was used as the pore former to produce the bioceramic scaffold. Bulk density, apparent porosity and compressive strength of the scaffold were calculated. Thereafter, characterization techniques like Mercury Intrusion Porosimetry and Scanning Electron Microscopy (SEM) were carried out to study the macro/micro pores and microstructure of the scaffold in detail. In the end, in-vitro bioactivity using SBF was done which was followed by a detailed SEM study of the SBF-treated scaffold which showed the growth of tissue over the scaffold surface.

1. INTRODUCTION

1.1 Bone

1.2 Bone Tissue Engineering

1.3 Scaffold Design

1.4 Present Project

1.4.1 Objective

1.4.2 Why use Hap for preparation of scaffold ?

1.1 Bone

Bone is a specialized connective tissue with mineralized extracellular marix (ECM). Bone grafting is routinely performed to restore bone loss due to trauma or disease. It is well known that hydroxyapatite (Hap) is the major component of natural bone mineral and has been found to possess good mechanical properties, biocompatibility, and osteoconductivity [1]. For these reasons, sintered Hap or other calcium phosphate apatites have been widely used for repair and replacement of damaged or traumatized bone tissues [2-4]. However, these materials have major disadvantages for tissue engineering applications: they are lack of desired degradability in a biological environment, are brittle, and their processing capacity into a predesigned highly porous structure is limited.

There is a growing need for bone regeneration due to various clinical bone diseases such as bone infections, bone tumors and bone loss by trauma [5]. Current therapies for bone defects include autografts, allografts, xenografts and other artificial substitutes such as metals, synthetic cements and bioceramics [6-7]. However, these substitutes are far from ideal and each has its specific problems and limitations. For example, autografts are associated with donor shortage and donor site morbidity whereas allografts and xenografts have the risk of disease transmission and immune response [8], and synthetic materials wear and do not behave like true bone.

1.2 Bone Tissue Engineering

Bone tissue engineering is an increasingly important research area whose goal is to surpass the limitations of conventional treatments based on organ transplantation and biomaterial implantation [9]. There are three general approaches in tissue engineering [10] :

- the use of isolated cells or cell substitutes to replace those cells that supply the needed function;
- the delivery of tissue-inducing substances, such as growth and differentiation factors to targeted locations;
- growing cells in three-dimensional scaffolds.

The third approach has seen significant research developments. Porous matrices, known as scaffolds, to which cells attach and colonize, play a vital role in synthesizing bone–extracellular matrix and associated biological molecules to facilitate the formation of functional tissues/organs. Scaffolds for bone regeneration should meet criteria to serve this function, these include [11] :

- ✓ a high porosity and appropriate pore size;
- ✓ a high surface area is required;

- ✓ biodegradability is generally required and a degradation rate is needed to match the rate of tissue formation;
- ✓ mechanical integrity to maintain the pre-designed tissue structure;
- ✓ biocompatibility (i.e. non-toxic to cells);
- ✓ the scaffold should display a positive interaction with cells, that may include enhanced cell adhesion, proliferation, migration, and differentiation;
- ✓ scaffolds are also used as carriers for the delivery of growth and differentiation factors, e.g., the factors can be adsorbed on the surface of the scaffold.

These scaffold requirements are extremely complex and tissue-specific to the structure and function of the host tissue. Creating scaffolds and engineering bone tissues that meet the needs of specific repair sites in particular patients is a major challenge in the field of bone tissue engineering research.

1.3 Scaffold Design

In bone regeneration, scaffolds serve as a template for cell interactions and formation of bone extracellular matrix to provide structural support to the newly formed tissue. Therefore, it is necessary that the scaffolds should, in some respects, mimic host bone morphology in order to optimise integration into surrounding tissue. *Porosity is defined as "the percentage of void space in a solid and it is a morphological property independent of the material"* [12]. Pores are necessary for bone tissue formation because they allow migration of endothelial cells: to promote osteoblasts or progenitor cells; to promote vascularisation of mesenchymal cells; or to facilitate osteoblast proliferation and differentiation (i.e. osteogenesis). In addition, a porous surface improves mechanical stability and interlocking at the critical interface between the implant biomaterial and the surrounding natural bone. The minimum pore size required to regenerate mineralized bone is generally considered to be approx. 100 µm after the study of Hulbert et al. [13].

Relatively larger pores favour direct osteogenesis, since they allow vascularisation and high oxygenation, while smaller pores result in osteochondral ossification although the type of bone in-growth depends on the biomaterial and the pore geometry. Moreover, porosity and pore size properties influence mechanical properties. An increase in the void volume results in a reduction in mechanical strength and stiffness of the scaffold, which can be critical for regeneration in load-bearing bones. The extent to which pore size can be increased while maintaining mechanical requirements, is dependent on a number of factors including the nature of the biomaterial and the processing conditions used in the fabrication of 3D scaffolds [14].

1.4 Present Project

1.4.1 Objective

The principal objectives of this project were as follows :

- To prepare phase pure Hap by co-precipitation method involving $CaNO_3.4H_2O$ and $(NH_4)_2HPO_4$.
- To achieve stability of the above Hap powder's calcined form at higher temperatures, upto 1250^0C.
- To prepare Hap scaffolds having various degrees of porosities and study their bulk densities and compressive strengths.
- To study the nature of pores in the scaffolds by studying their porosimetry curves and microstructures.
- To study the changes on the surface of the scaffolds after treating them with SBF for considerable amount of time.

1.4.2 Why use Hap for preparation of scaffold ?

Hydroxyapatite $[Ca_{10}(PO_4)_6(OH)_2]$ is one of the most biocompatible ceramics because of its significant chemical and physical resemblance to the mineral constituents of human bones and teeth. It is a bioactive ceramics widely used as powders or in particulate forms in various bone repairs and as coatings for metallic prostheses to improve their biological properties. It has excellent biocompatibility, bioactivity and osteoconduction properties. Hap is thermodynamically the most stable calcium phosphate ceramic compound nearest to the pH, temperature and composition of the physiological fluid.

Due to the chemical similarity between Hap and mineralized bone of human tissue, synthetic Hap exhibits strong affinity to host hard tissues. Formation of chemical bond with the host tissue offers Hap a greater advantage in clinical applications over most other bone substitutes, such as allograft or metallic implants.

Porous Hydroxyapatite

Porous Hap exhibits strong bonding to the bone; the pores provide a mechanical interlock leading to a firm fixation of the material. Bone tissue grows well into the pores, thus increasing strength of the Hap implant. The ideal bone substitute is a material that will form a secure bond with the tissues by allowing, and even encouraging, new cells to grow and penetrate [14].

One way to achieve this is to use a material that is osteophilic and porous, so that new tissue, and ultimately new bone, can be induced to grow into the pores and help to prevent loosening and movement of the implant. A porous hydroxyapatite coating facilitates bone growth through a highly convoluted interface. When pore sizes exceed 100 μm, bone grows through the channels of interconnected surface pores, thus maintaining the bone's vascularity and viability. Since porous Hap is more resorbable and more osteoconductive than dense Hap, there is an increasing interest in the development of synthetic porous hydroxyapatite (Hap) bone replacement materials for the filling of both load-bearing and non-load-bearing osseous defects. Simulating the human bone structure, porous Hap scaffold has large surface area, which is beneficial for adhesion of biological tissue cell and growth of new bone phase [15].

2. LITERATURE SURVEY

2.1 Bioceramics - A subset of Biomaterials

2.2 Hydroxyapatite

2.3 Bioceramic Scaffolds

2.4 Processing Bioceramic Materials

2.1 Bioceramics – A subset of Biomaterials

The first generation of inert ceramics aimed to substitute natural bone, hence the research was only focused on inert materials; the second one was aimed at mimicking some biomineralization-related functions and sol-gel chemistry plays a paramount role in their synthesis and properties. Finally, the purpose with third generation bioceramics is basically to provide an adequate scaffolding system which helps the bone cells to perform their natural processes [16].

Imperial Roman empire folks had a very low life expectancy of just 22 years which almost doubled to 40 years by the early 20^{th} century and now we are comfortably boasting of a great 80 years of life expectancy by the end of this 20^{th} century. Biomaterials have made all the difference. If we focus on functional artificial biomaterials, the choice has to be made among metals, polymers and ceramics. Each group exhibits some a priori advantages and drawbacks. Ceramics, for instance, are the most biocompatible materials and can be obtained with biostable, bioactive or bioresorbable properties, but their main drawbacks are their hardness and fragility. Metals exhibit problems of corrosion and toxicity, but their mechanical behavior is optimum. Polymers offer many possibilities depending on their chemical composition and structure (biodegradability degree, hydrophilic/ hydrophobic ratio, toughness/flexibility, etc.), but very few have shown good bioactive properties (for instance, Poliactive1) to ensure the implant osteointegration. Therefore, it is important to reach the best compromise possible, and it is quite usual to use the three types of materials in the same implant. This is the case of a total hip joint prosthesis which presents a metal beam, partially coated with a bioactive ceramic, while the head is made of an inert ceramic and the socket is made of polymer [17].

2.2 Hydroxyapatite

The inorganic phase of our bones is apatite. Apatite is the term of a very abundant mineral in the earth's crust, with $Ca_{10}(PO_4)_6(OH)_2$, {more commonly known as Hydroxyapatite (Hap)} as general formula [18]. Its structure has the special ability to accommodate several different ions in its three sublattices [19,20]. Bone apatites can be considered as basic calcium phosphates. Biological apatites are formed in living bodies through a biomineralisation process where cells and proteins are involved.

2.3 Bioceramic Scaffolds

In order to work in potential hard tissue replacement solutions, it is required to know and bear in mind the bone regeneration process. Wolf's law dictates that the bone remodels itself as a function of

those forces acting on it, hence preserving its shape and density. The mechanical loads of stress, compression, flex and torsion in bones and the interstitial fluid contained in them generate stresses and deformations at the microscopical level, which in turn stimulate the cells [21].

The fabrication of scaffolds for tissue engineering requires choosing a conformation method that yields pieces with interconnected porosity and pores in the 20 to 400 micron range [22]. The main purpose now is to obtain porous ceramics that act as scaffolds for cells and inducting molecules, able to drive self-regeneration of tissues.

Polymer scaffolds were used as negative of the desired ceramic piece. After conforming the piece, the polymer is removed by an acid or basic attack, or using mild temperatures. These pieces, with designed porosity, preserve their bioactive behavior, where apatite has grown throughout all the free surfaces [23, 24].

An important challenge is to design materials that can help the human body to improve its regeneration features, not only recovering the structure of the damaged tissue, but also its function [25]. Tissue engineering aims to restore the structure and function of the tissues or damaged organs. The repair starts by in vitro techniques on scaffolds cultured with cells, to be then implanted in the host [26].

2.4 Processing of Bioceramic Materials

Sopyan et al. [27] studied porous hydroxyapatite for artificial bone applications. It was reported that the preparation of Hap porous bodies via polymeric sponge method; the samples of which were prepared using sol–gel method-derived Hap powders and commercial Hap powders showed a considerable compressive strength ranging from 1.3 to 10.5 MPa for the increased apparent density from 1.27 to 2.01 g/cm^3. This was higher than the 0.55–5 MPa compressive strength obtained for the apparent densities of 0.0397– 0.783 g/cm^3, as reported by Ramay et al. [28]. It was also shown that homogeneity of slurry and heating rate affected porosity and density of porous bodies, in turn influencing the compressive strength. More homogeneous slurries and faster heating rate gave porous bodies with the increased compressive strength due to higher apparent density and crystallinity.

Potoczek [29] studied the gel casting of hydroxyapatite foams using agarose as gelling agent and the rheological behavior of the suspensions. The viscosity of the slurries could be adjusted by agarose concentration and Hap solid loading. These parameters were essential in tailoring the porosity as well as the cell and window sizes of the resulted Hap foams. Depending of Hap solid loading (24–29 vol.%) and agarose concentration (1.1–1.5 wt.% with regard to water) in the starting slurry, the mean cell size ranged from 130 to 380 μm, while the mean window size varied from 37 to 104 μm. Depending on the porosity

range (73–92%) and related with this parameter the mean cell and window size, the compressive strength of Hap foams was found to be in the range 0.8–5.9 MPa.

Schwartzwalder and Somers [30] studied the slurry infiltration process for making porous ceramics. In this process poly urethane (PU) foam was infiltrated with ceramic slurry and the body was compressed by passing it through a set of rollers to remove the excess slurry. In this manner the slurry remained coated on the PU struts and open pore channels were left in between. The coated PU perform was then dried, followed by burn out of the PU and sintering at higher temperature. The foams produced were reticulated foams with porosity within the range 75-90%.

Thijs et al. [31] studied a novel technique to produce macroporous ceramics using seeds and peas as sacrificial core materials. The first step in this technique was to coat the seeds, peas with wetting ceramic slurry that undergoes gelation. The coated seeds and peas were consolidated by packing them in a container and infiltrating with ceramic slurry which underwent gelation. The compacts thus obtained were subjected to the conventional steps of drying, binder burn out and sintering. The resulting bodies had greater than 90% porosity with pore size determined by the size of the seeds, peas.

Itatani K et al. [32] studied the preparation of Porous Hydroxyapatite Ceramics from Hollow Spherical Agglomerates Using a Foaming Agent of H_2O_2 and observed that by changing the concentration of H_2O_2 solution from 0 to 20 mass%, the total porosity of Hap compact fired at 1000^0C for 5 hrs could be changed linearly from 61.2 to 71.7%. The Hap compact exhibited pore sizes with maximum porosity (71.7%) at around 0.7 μm, 5-100 μm and 100-200 μm.

Soon-Ho kwon et al. [33] successfully fabricated porous bioceramics with variable porosity, using the poly urethane sponge technique. Porosity was controlled by the number of coatings on the sponge struts. When a porous body was produced by a single coating, the porosity was ~90%, and the pores were completely interconnected. When the sintered body was coated five times after the porous network had been made, the porosity decreased to 65%. The compressive strength was strongly dependent on the porosity and weakly dependent on the type of ceramics, Hap, TCP, or Hap/TCP composite. At the 65% porosity level, the strength was ~3 MPa. The TCP exhibited the highest dissolution rate in a Ringer's solution, Hap had lowest rate. The biphasic Hap/TCP showed an intermediate dissolution rate. The biodegradation of calcium phosphate ceramics could be controlled by simply adjusting the amount of Hap or TCP in the ceramic. Han Guo et al. [34] studied biocompatibility and osteogenicity of degradable Ca-deficient hydroxyapatite (CaD Hap) scaffolds from calcium phosphate cement for bone tissue engineering by a particle leaching method. The morphology, porosity and mechanical strength as well as degradation of the scaffolds were characterized. The results indicated that the CaD Hap scaffolds with a porosity of 81% showed open macropores with pore sizes of 400–500 μm. Thirty-six per cent of these CaD Hap scaffolds were degraded after 12 weeks in Tris–HCl solution. The results revealed that the CaD Hap scaffolds were biocompatible and had no negative effects on the mesenchymal stem cells (MSCs) in

vitro. The in-vivo biocompatibility and osteogenicity of the scaffolds were investigated. The CaD Hap scaffold after 8 week implantation shows good biocompatibility and extensive osteoconductivity.

Deville et al. [35] studied the freeze casting of porous hydroxyapatite scaffolds and observed that by varying the freezing rate of slurry as well as slurry concentration, porosities in the range 40-60% could be achieved. The pores were open and unidirectional and exhibited a lamellar morphology. The processed scaffolds exhibited high compressive strength up to 145 MPa.

Xiao Huang et al. [36] studied the Hap-based composite scaffolds that have a unique macroporous structure and special struts of a polymer/ceramic interpenetrating composite. A novel combination of polyurethane (PU) foam method and a hydrogen peroxide (H_2O_2) foaming method is used to fabricate the macroporous HA scaffolds. Micropores are present in the resulting porous Hap ceramics after the unusual sintering of a common calcium phosphate cement and are infiltrated with the poly(D,L-lactic-co glycolic acid) (PLGA) polymer. The internal surfaces of the macropores are further coated with a PLGA bioactive glass composite. It is found that the HA scaffolds fabricated by the combined method show high porosities of 61–65% and proper macropore sizes of 200–600 μm. The PLGA infiltration improved the compressive strengths of the scaffolds from 1.5–1.8 to 4.0– 5.8 MPa.

3. EXPERIMENTAL PROCEDURE

3.1 Preparation of Hydroxyapatite

3.1.1 Estimation of Calcium Nitrate Tetrahydrate

3.1.1.1 Reactions

3.1.2 Batch Calculations

3.1.3 Synthesis of Hydroxyapatite

3.1.3.1 Procedure

3.1.3.2 Reactions

3.1.4 Flowchart

3.2 Characterisations of synthesized and calcined Hap

3.3 Preparation of Hap Scaffold using PEG-600

3.4 Characterisations of Hap Scaffold

3.5 Bioactivity of Hap Scaffold using SBF

3.1 Preparation of Hydroxyapatite

Solution-precipitation method, also known as Co-Precipitation Method was applied using $Ca(NO_3)_2 \cdot 4H_2O$ (Merck, India) and $(NH_4)_2HPO_4$ (Merck, India) as the starting materials and Ammonia (NH_3) solution(Merck, india). A solution of 1M $Ca(NO_3)_2 \cdot 4H_2O$ was prepared at 25^0C.

3.1.1 Estimation of {$Ca(NO_3)_2.4H_20$}

3 ml of $Ca(NO_3)_2.4H_20$ was pipette out into a beaker and it was titrated against 2.5 M NaOH solution. The precipitate was filtered and the residue was calcined at 1000^0C at a rate of 3^0C/min. for 2 hours.

Calculations :

Wt. of empty Al_2O_3 crucible – 1 – 140.0463 gm (W_{E1}).

Wt. of empty Al_2O_3 crucible – 2 – 152.7539 gm (W_{E2}).

Wt. of empty Al_2O_3 crucible – 3 – 136.0114 gm (W_{E3}).

Wt. of (sample + crucible) – 1 – 140.1694 gm (W_{S1})

Wt. of (sample + crucible) – 2 – 152.8769 gm (W_{S2})

Wt. of (sample + crucible) – 3 – 136.1349 gm (W_{S3})

Wt. of CaO – 1 – $W_{S1} – W_{E1}$ = 140.1694 – 140.0463 = 0.1231 gm.

Wt. of CaO – 1 – $W_{S2} – W_{E2}$ = 152.8769 – 152.7539 = 0.1230 gm.

Wt. of CaO – 1 – $W_{S3} – W_{E3}$ = 136.1349 – 136.0114 = 0.1235 gm.

3 ml of $Ca(NO_3)_2.4H_2O$ contain CaO = {(0.1231 + 0.1230 + 0.1235) / 3} gm = 0.1232 gm.

So, 1 ml of $Ca(NO_3)_2.4H_2O$ contains CaO = 0.1232 / 3 = 0.0411 gm.

- ⇨ 0.0411 gm of CaO from 1 ml of $Ca(NO_3)_2.4H_2O$
- ⇨ 1 gm of CaO from (1 / 0.0411) ml of $Ca(NO_3)_2.4H_2O$ = 24.3309 ml.

3.1.1.1 Reactions

$$Ca(NO_3)_2 + 2NaOH \longrightarrow Ca(OH)_2 + 2NaNO_3$$

$$Ca(OH)_2 \xrightarrow{850^0C,\ 2hrs\ /\ 3^0C\ /\ min^{-1}} CaO + H_2O$$

3.1.2 Batch Calculation

We tested a 10 gm batch. Hydroxyapatite is given by the formula $Ca_{10}(PO_4)(OH)_2$ (Hap).

Ca / P ratio = 10/6 = 1.67

For 1 mole of Hap → 6 moles of phosphate required.

Molecular Wt. of $(NH_4)_2HPO_4$ = 132.06 gm

Molecular Wt. of Hap = 1004 gm

Therefore 1004 gm of Hap requires 6 x 132.06 gm of phosphates = 792.36 gm of phosphates

- ⇨ 10 gm of Hap requires {(792.36 / 1004) x 10} = 7.8884 gm of $(NH_4)_2HPO_4$.

NH_4OH = 480 ml (1:1) solution.

$(NH_4)_2HPO_4$ = 7.8884 gm / 40 ml of distilled H_2O.

CaO required = {1.67 x 7.8884 x 56.08} / 132.06 = 5.5943 gm

Total $Ca(NO_3)_2.4H_2O$ required = (5.5943 x 24.3309) ml = **136.1144 ml.**

3.1.3 Synthesis of Hydroxyapatite

3.1.3.1 Procedure

The Ca:P ratio for stoichiometric HA =1.67. Keeping that ratio constant, the amount of $(NH_4)_2HPO_4$ required was calculated and it was prepared by dissolving $(NH_4)_2HPO_4$ in distilled water. The prepared solution of $(NH_4)_2HPO_4$ was slowly added to the $Ca(NO_3)_2.4H_2O$ solution (in stirring condition) resulting in the formation of a turbid solution. Conc. HNO_3 was added and the resulting solution was shaken well for a few minutes till a colourless solution was obtained. Then 1:1 NH_3 solution (NH_4OH) was added drop wise and stirred and continuously till the Hap white precipitate was formed. The pH in the entire experiment was maintained at 10.4. The Hap ppt. was stirred (magnetic stirrer) for 2-3 hours and the precipitate was aged for overnight for settling of the precipitates followed by decantation and removal of ammonia by repeated washing of the precipitate with distilled water.

The settled material was centrifuged with the help of a High – Speed Centrifuger (rotational speed of 8000 rpm). The ppt. left out was dried at 85^0C for 24 hours and then the dried mass was calcined at 850^0C for 2 hrs at 3^0C/min.

3.1.3.2 Reaction

$$10Ca(NO_3)_2.4H_2O + 6(NH_4)_2HPO_4 + 8NH_4OH \rightarrow Ca_{10}(PO_4)_6(OH)_2 + 20NH_4NO_3 + 46H_2O$$

3.1.4 Flowchart of Hap synthesis

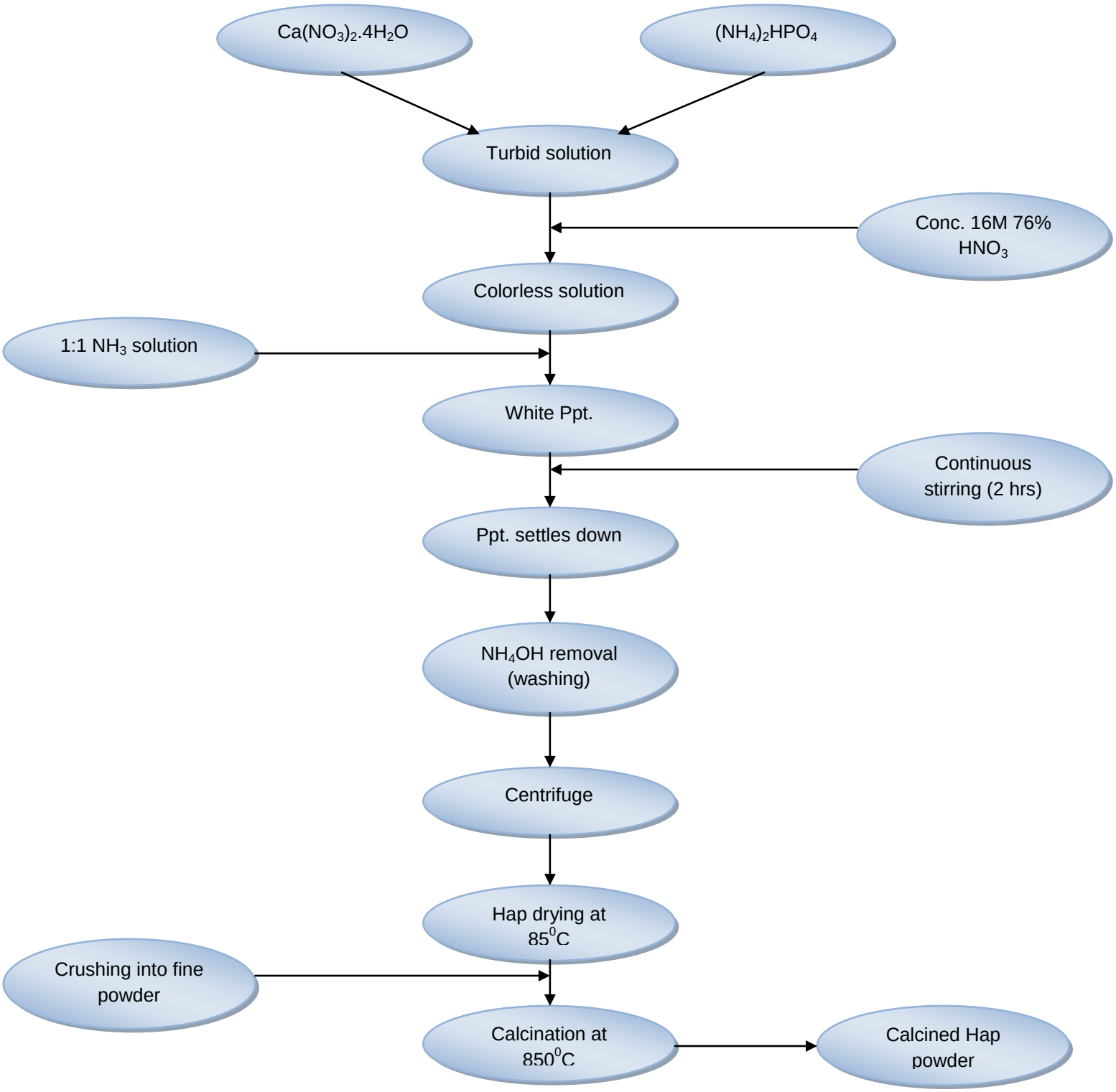

3.2 Characterisations for synthesized and calcined Hap

The following characterizations were done after calcinations of Hap powder :

- ✓ X-Ray Diffraction (XRD) Analysis of calcined Hap by PANAnalytical XRD machine from Philips, Netherlands. The incident angle (Θ) varied between 20^0 and 80^0. λ of Cu K_α radiation was 1.54 A^0. The Hap peaks were identified using JCPDS file (reference number – 74-0565).
- ✓ Fourier Transform InfraRed Spectroscopy (FTIR) of synthesized and calcined Hap by FTIR instrument of Perkin-Elmer.
- ✓ BET Analysis of synthesized and calcined Hap by BET machine of Quantachrome, USA.
- ✓ Particle Size Analysis of both synthesized and calcined Hap by Zetasizer Nano Series, Nano ZS of MALVERN.

3.3 Preparation of Hap Scaffold using PEG-600 (Pore Former)

The objective was to prepare bioceramic Hap scaffolds each with a different amount of porosity. Hence required amounts (as given in the following table) of calcined Hap powder and Polyethylene Glycol (PEG – 600), here 600 being the molecular mass of PEG used in this project, were first taken and mixed after weighing in the required materials using an electronic weighing machine.

Table 3.1. Weights of Calcined Hap and PEG – 600 used to prepare Hap scaffolds.

Wt. of Calcined Hap (gms)	Wt. of PEG – 600 (gms)
1	0.48
1	0.52
1	0.60
1	0.80
1	1.40
1	2.40

Mixing was done using a mortar and pastel. Three samples of each mixture were taken and pelletized using the Carver Pelletising Machine at a pressure of 5 Tonnes for 2 mins.

The pellets were then dried at 85^0C for 24 hours and then sintered at 1250^0C keeping the soaking time as 4 hours to produce the required scaffolds.

3.4 Characterizations of Hap Scaffold

A few measurements and characterizations were done of the scaffolds which were produced.

Measurements :

- **Bulk Density (B.D.) and Apparent Porosity (A.P.)** by wet – analysis method (Archimedes' Principle).

  B.D. and A.P. of scaffold was measured by applying Archimedes' principle. Dry weight of sample was taken then samples were kept inside a beaker filled with kerosene and it was kept inside a desiccator for half an hour. Then suspended as well as soaked weight of samples was taken.

  A.P. and B.D. were represented as :

  A.P. (%) = {(W – D) / (W – S)} x 100

  B.D. (g/cc) = {D / (W – S)} x d

  Where, W = Soaked weight of the sample,

  S = Suspended weight of the sample,

  D = Dry weight of the sample,

  d = Density of kerosene (0.81 g/cc).

- **Compressive Strength**

The compressive strength of the sintered samples was measured by universal testing machine (H10 KS TINIUS OLSEN). The circular pellets (diameter d, thickness t) were broken in compression. The compressive strength of the pellets was determined from the following formula :

For circular pellets :

Compressive Strength (σ) = (2 x P) / (π x d x t),

Where P = load in kN,

d = diameter of pellet,

t = thickness of pellet.

Characterisations :

- **Porosimetry** using Mercury Intrusion Porosimeter.
- **Scanning Electron Microscopy (S.E.M.)** using JEOL JSM – 6480 LV SEM and EDAX machine (Pt coating of 20 A^0 on each sample using JEOL JFC – 1600 Auto Fine Coater).

3.5 Bioactivity of Hap Scaffold using SBF

Each scaffold pellet (one each of different porosities) was dipped in SBF (Simulated Body Fluid) solution and kept in the B.O.D. incubator at 37^0C and pH = 7.4 for 33 days. The SBF solution was replenished every 7 days.

Table 3.2 SBF composition [38] :-

Sl. No.	Reagent	Amount (gms/litre)
1	NaCl	6.547
2	$NaHCO_3$	2.268
3	KCl	0.373
4	$Na_2HPO_4.2H_2O$	0.178
5	$MgCl_2.6H_2O$	0.305
6	$CaCl_2.2H_2O$	0.368
7	Na_2SO_4	0.071
8	$(CH_2OH)_3CNH_2$	6.057

The samples were taken out, dried for 12 hours and then another SEM study was done of these SBF – treated pellets to study the surface changes in the scaffolds.

Details of all of the above mentioned measurements and characterizations are given in the next section of this thesis.

4. RESULTS & DISCUSSIONS

4.1 Hydroxyapatite Characterizations

4.1.1 XRD Analysis of Hap

4.1.1.1 Synthesized Hap

4.1.1.2 Calcined Hap

4.1.1.3 Sintered Hap

4.1.1.4 Particle size Calculation

4.1.2 FTIR of Hap Synthesized

4.1.3 BET Analysis of Hap Calcined

4.2 Hap Scaffolds' Characterizations

4.2.1 Apparent Porosity and Bulk Density

4.2.2 Compressive Strength

4.2.3 SEM of Hap Scaffolds

4.2.4 Pore Distribution Analysis

4.2.5 In-Vitro Bioactivity

4.2.5.1 SEM

4.2.5.2 EDAX

4.1 Hydroxyapatite Characterizations

4.1.1 X-Ray Diffraction (XRD) Analysis of Hap

4.1.1.1 Synthesized Hap

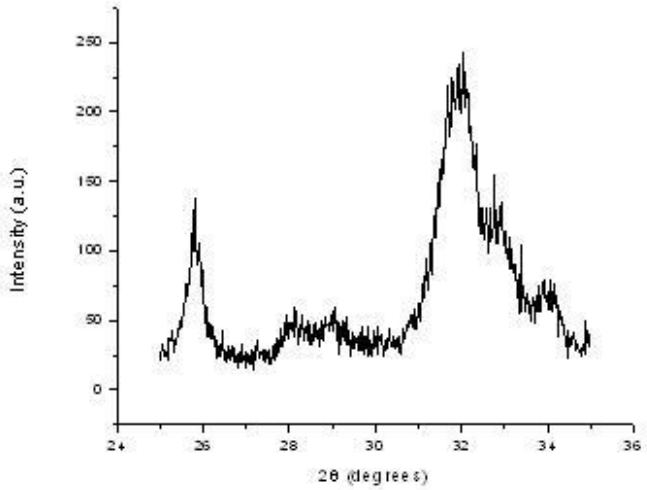

Fig. 4.1 XRD pattern of synthesized Hap

4.1.1.2 Calcined Hap

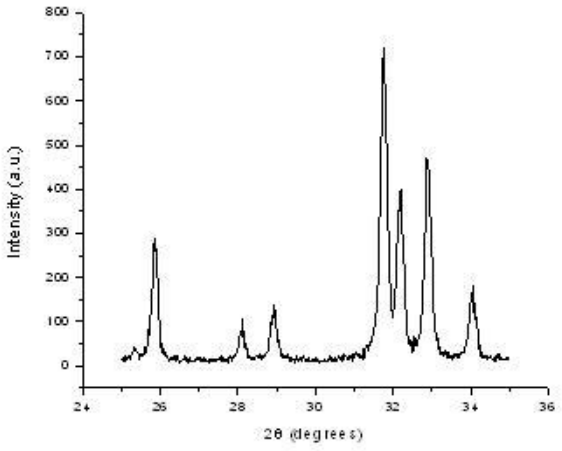

Fig. 4.2 XRD pattern of calcined Hap at 850^{0}C

4.1.1.3 High Temperature XRD of calcined Hap

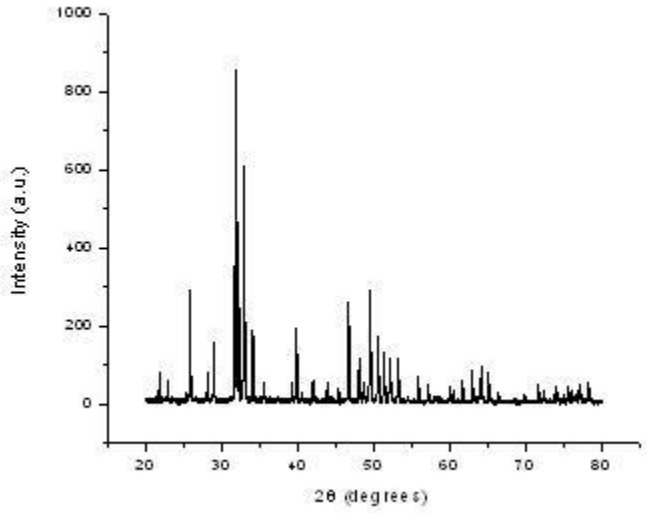

Fig. 4.3 XRD pattern of Hap at 1250^{0}C

Fig. 4.1, Fig. 4.2 and Fig. 4.3 show the XRD patterns of synthesized Hap, calcined Hap (850^{0}C) and high temperature stability behavior of Hap at 1250^{0}C prepared by co-precipitation method. The Hap peaks were identified by referring JCPDS files (Ref No. 74-0565).

The XRD pattern shows that the calcined powder contains only hydroxyapatite. No extra peaks were found. Thus the synthesized Hap powder was phase pure upto 1250^{0}c without decomposition to β-TriCalcium Phosphate (TCP). The peaks were sharper as the synthesized powder was calcined and in the end, sintered. It showed that the crystallinity of the powder increased at each following step.

4.1.1.4 Crystallite size calculation

We know that

$t = (0.96 \times \lambda) / (\beta \times \cos \theta)$, where t = particle size,

λ = wavelength of K_α – Cu used = 1.54 A^0

β = Full Width Half Maximum (FWHM)

Θ = Incident Angle

So, t = {0.96 x 1.54} / {0.001373 x cos (31.8019 / 2)}

= 1120 A^0 = **112 nm**.

4.1.2 Fourier Transform Infrared Spectroscopy (FTIR)

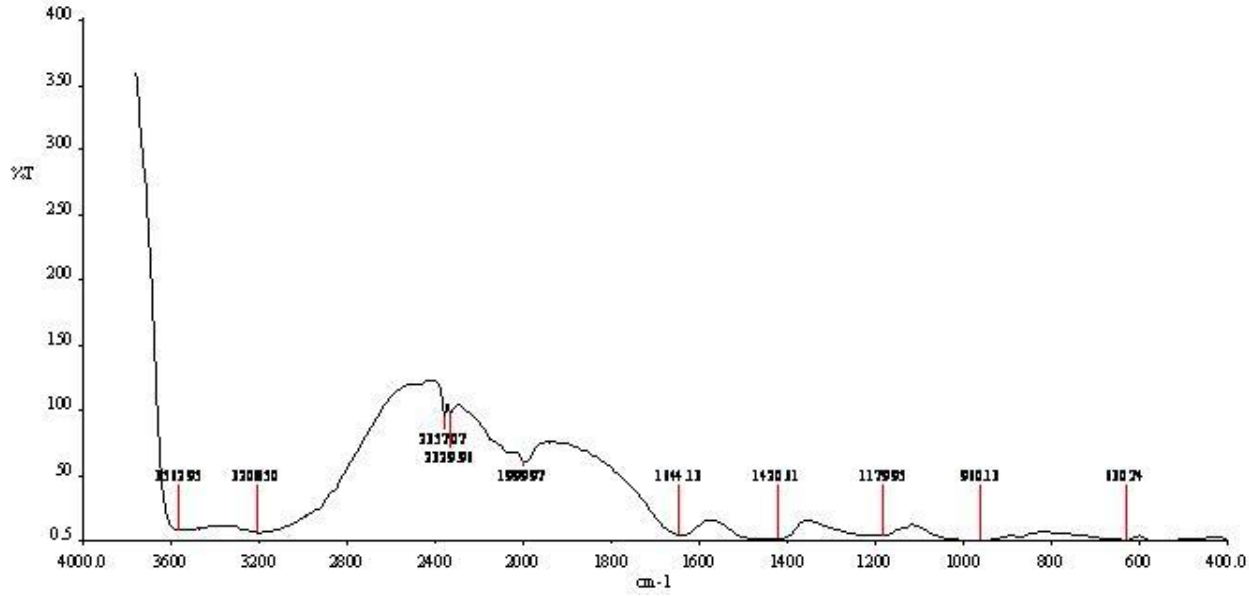

Fig. 4.4 FTIR pattern of synthesized Hap

Table 4.1 Wavenumbers corresponding to their respective functional groups in FTIR spectroscopy

Wave number (cm^{-1})	Functional Group
3562.95	OH -
2357.07, 2329.94	CO_3^{2-} (C=O)
1179.95	C - O
1644.13, 1420.61	NO_3^-
960.13, 630.74	PO_4^{3-}

Wavenumbers greater than 1400 cm^{-1} constitute the stretched bands and less than 1400 cm^{-1} are the bending bands of the functional groups. Thus it was seen that OH – and PO_4^{3-} functional groups were least transmitted denoting their large presence in the material tested (Hap here).

4.1.3 Surface Area Analysis of Hap

BET Equation :

$$1 / [v \{ (P_0/P) – 1] = \{ (c – 1) / v_m \times c\} + 1 / (v_m \times c)$$

where, v = adsorbed gas quantity (volume units),

P = equilibrium pressure of adsorbate,

P_0 = saturation pressure of adsorbate,

c = BET constant,

v_m = monolayer adsorbed gas quantity.

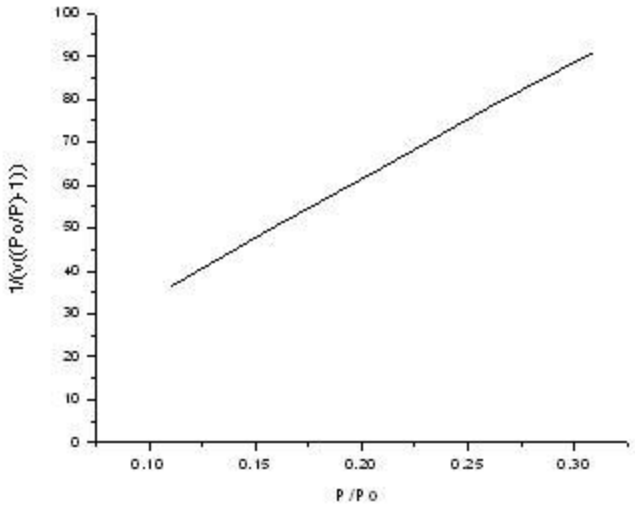

Fig. 4.5 BET plot

From this plot, we find the following details :

Slope of the plot = A = 276.2,

Y – intercept = I = 6.034.

So, calculating v and c, we have :-

v = {1 / A + I} c = {1 + (A / I)}

= {1 / (276.2 + 6.034)} = {1 + (276.2 / 6.034)}

= 3.54×10^{-3}. = 46.77

Now, we know that

$\mathbf{S_{total} = (v_m \times N_A \times s) / V}$ where, N_A = avogadro's Number, a = mol. Wt.(adsorbed species)

$\mathbf{S_{BET} = S_{total} / a}$ s = adsorption cross-section.

So, S_{total} = {$3.54 \times 10^{-3} \times (6.22 \times 10^{23}) \times (16.2 \times 10^{-20})$} / 0.8865}

= 403.02 m^2.

Hence S_{BET} = 403.02 / 28.0134 = 12.34 m^2/g.

We found the particle size (t) by the following formula :

$$t = \{ 6 / (\rho \times S_{BET})$$

$= \{ 6 / (3.16 \times 12.34)$

$= 0.15387\ \mu m$

$=$ **153.87 nm**.

The particle size found by the above mentioned BET method varied slightly with the data obtained from the ***Paticle Size Analyzer (PSA)*** value which stood at **121.8 nm.**

4.2 Hap Scaffolds' Characterizations

4.2.1 Apparent Porosity and Bulk Density

The following table gives the values of Apparent Porosity and Bulk Density of various scaffolds prepared by varying the calcined Hap / PEG – 600 ratio.

Table 4.2 Apparent Porosity and Bulk Density of Hap scaffolds containing various concentrations of pore former PEG – 600.

Wt. of Hap (gms)	Wt. of PEG (gms)	Apparent Porosity (%)	Bulk Density (g/cc)
1.0	0.48	9.80	2.8563
1.0	0.52	20.67	2.4811
1.0	0.60	48.16	1.6410
1.0	0.80	54.73	1.4347
1.0	1.40	66.32	1.0659
1.0	2.40	76.07	0.7387

The above data show that increase in pore former amount (PEG -600) leads to increase in the apparent porosity of the scaffold but it is simultaneously accompanied with decrease in its bulk density. Pore formation is followed by the mechanism of diffusion of pore former PEG-600.

4.2.1 Compressive Strength (C.S.)

It is calculated by the formula :-

C.S. = (2 x P) / (π x d x t)

Table 4.3 Compressive Strengths of Hap scaffolds containing various concentrations of pore – former PEG – 600.

Wt. of Hap (gms)	Wt. of PEG (gms)	Diameter d (mm)	Thickness t (mm)	Load P (N)	Compressive Strength (MPa)
1.0	0.48	9.22	2.25	289	8.873
1.0	0.52	8.80	2.22	98	3.809
1.0	0.60	10.36	1.93	117	1.864
1.0	0.80	10.32	1.97	93.3	1.462
1.0	1.40	9.94	2.69	57	0.679
1.0	2.40	9.96	1.96	11	0.179

The above table clearly denotes that more the amount of pore-former, more is the porosity and hence, less is the compressive strength.

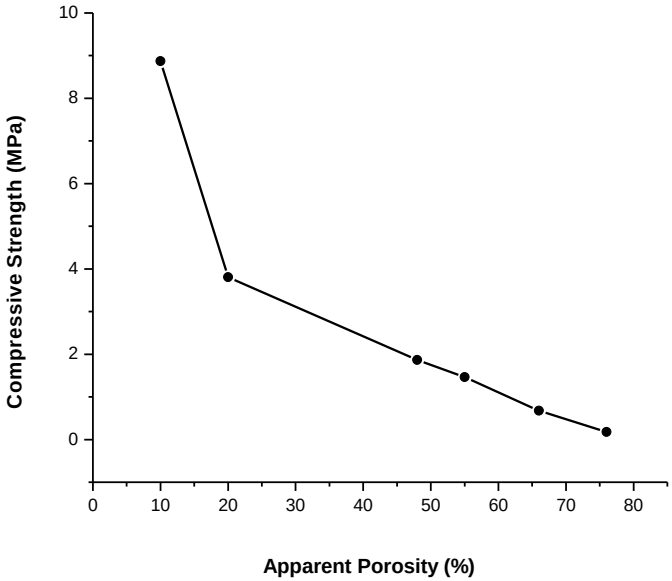

Fig. 4.6 Change of compressive strength w.r.t apparent porosity

Fig. 4.6 above shows that compressive strength decreases with increase in porosity as more porosity leads to loss of matter content and hence the loss in the strength of the sample(s).

4.2.3 SEM of Hap Scaffolds

Microstructures of the Hap scaffolds prepared by Co-Precipitation Method were studied from the Scanning Electron Microscopy (SEM) images as shown below.

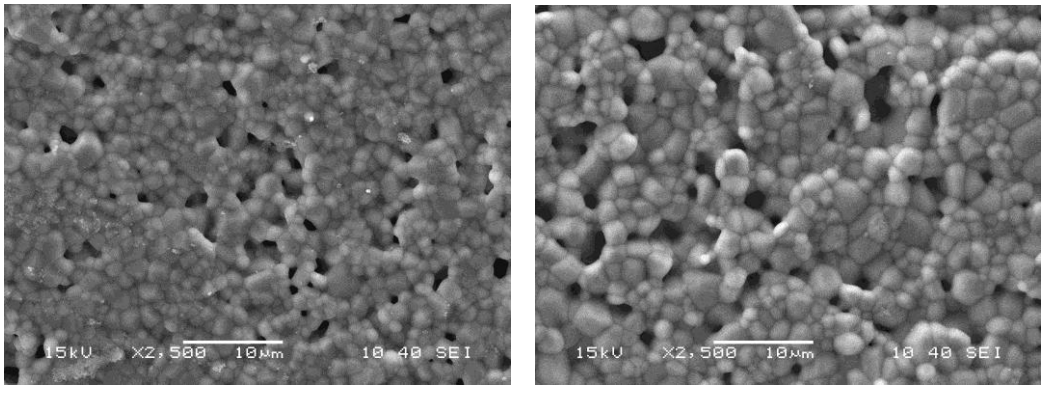

(a) **(b)**

Fig. 4.7 SEM images of Hap scaffolds prepared by Co-Precipitation Method. (a) 9.80% porosity, (b) 20.67% porosity.

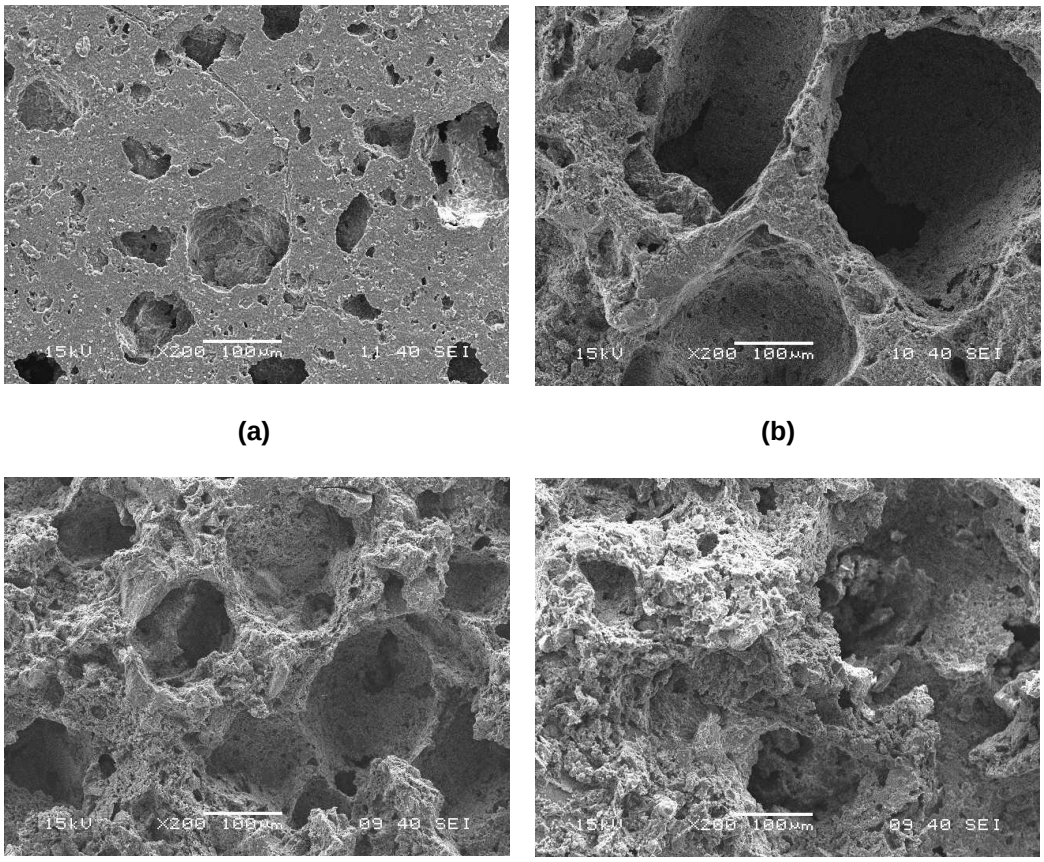

(a) **(b)**

(c) **(d)**

Fig. 4.8 SEM images of (a) 48.16%, (b) 54.73%, (c) 66.32%, (d) 76.07% porous scaffolds

It was seen that both macropores and micropores were interconnected. As the porosity increased, the number of interconnected pores increased. The pores were in the order of 100 – 400 µm. It was also seen that the size of the pores increased as the porosity increased.

So, although increase in porosity lead to increase in the pore-size but it decreased the total number of pores in a cross-section as clearly seen in the SEM images of Fig. 4.8.

4.2.4 Pore Distribution Analysis

Porosimetry was done for the scaffold with 48% porosity and its pore distribution analysis was done.

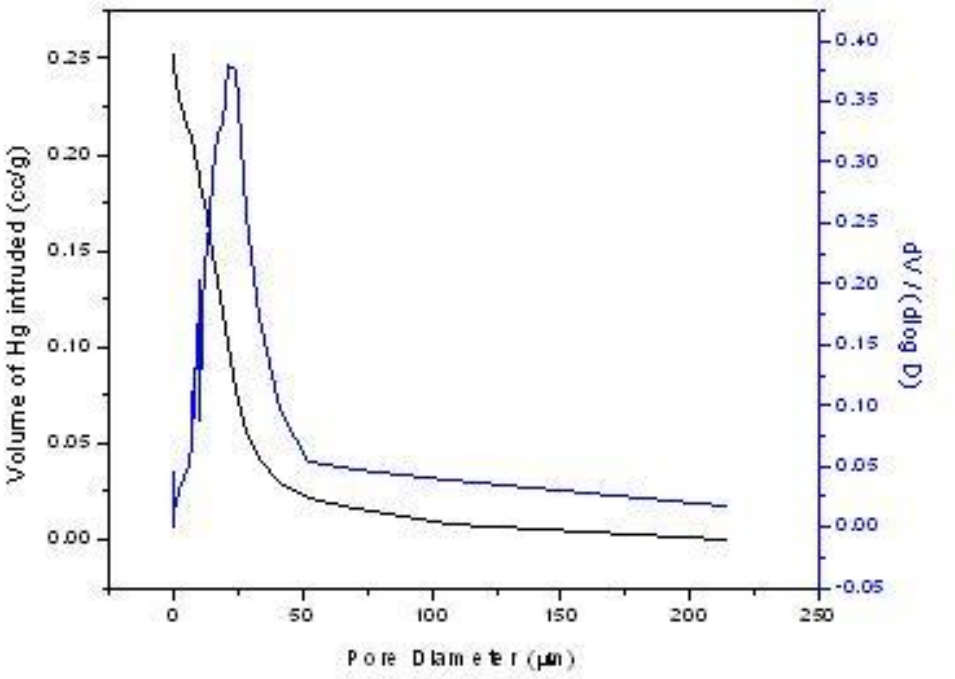

Fig. 4.9 Hg-intrusion study with respect to pore diameter in the scaffold with 48.16% porosity

Larger pores with pore diameter greater than 200 µm were analyzed by SEM study which follows this discussion here. However, Mercury Intrusion Porosimeter detected the content of smaller pores within the range of 2 – 50 µm.

4.2.5 In-Vitro Bioactivity

4.2.5.1 SEM

When porous Hap was treated in SBF solution, the mechanism which followed was presumably along the lines as discussed by Huang et al [36], who believed that at **first**, on soaking in SBF, the surface structural change occured in Hap resulting in the formation of a Ca-rich Amorphous Calcium Phosphate (ACP) on their surfaces. In view of change in Ca/P ratio, the formation of Ca-rich ACP was a consequence of interaction of the Hap surface, specifically with the calcium ions in the SBF. The **second** surface structural change was the formation of Ca-poor ACP, for which the Hap appeared to use the Ca-rich ACP on their surfaces to interact with the phosphate ions in the fluid. The **third** surface structural change was the formation of apatite. The Ca-poor ACP on the Hap appeared to gradually crystallize into bonelike apatite, through which the Hap appeared to stabilize their surfaces in SBF.

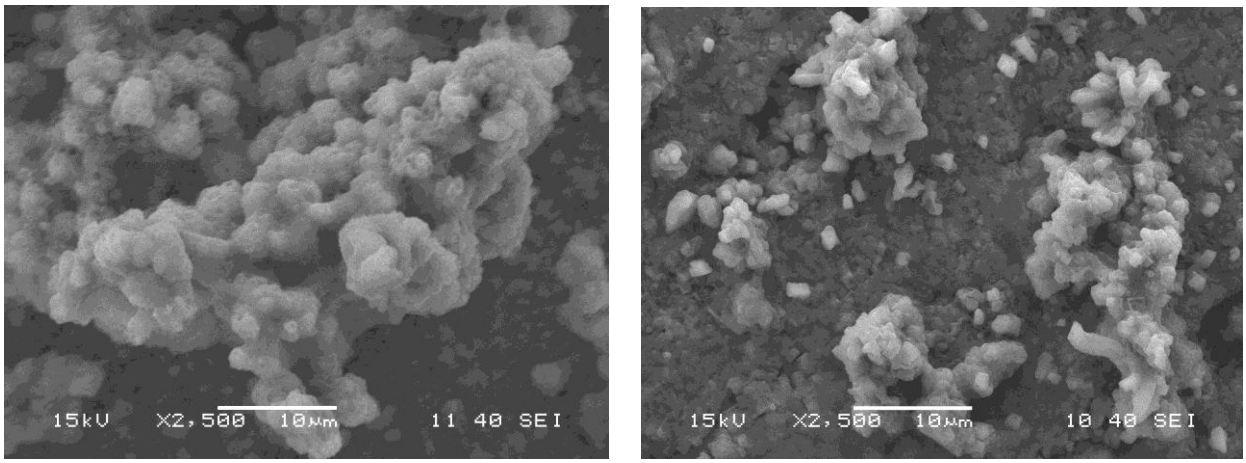

(a) **(b)**

Fig. 4.10i SEM images of SBF-treated Hap scaffolds prepared by Co-Precipitation Method.

(a) 9.80%, (b) 20.67% porosity.

The SEM of Hap scaffolds after being soaked in SBF solution for 33 days showed that carbonated Hap grew on the surface of porous scaffold and tissue growth was highly prominent in all the samples of varied porosities. The growth of carbonated Hap took place so rapidly in porous Hap scaffolds due to the presence of high degree of interconnectivity among the pores present in the samples.

Whereas in dense Hap materials, tissue growth is much slower because their specific surface areas are much lower in value as compared to their porous counterparts.

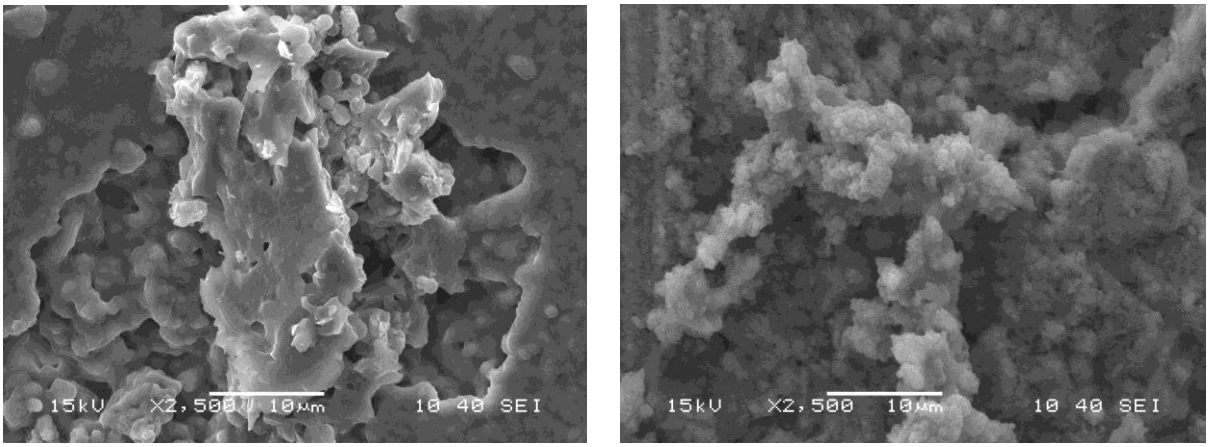

(a) **(b)**

Fig. 4.10ii SEM images of SBF-treated Hap scaffolds prepared by Co-Precipitation Method.

(a) 48.16%, (b) 54.73% porosity.

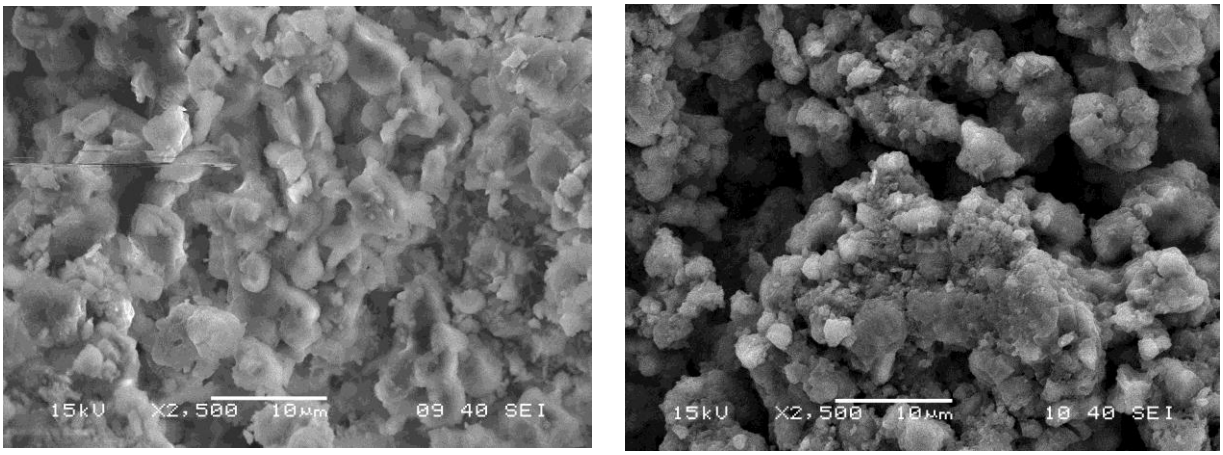

(a) **(b)**

Fig. 4.10iii SEM images of SBF-treated Hap scaffolds prepared by Co-Precipitation Method.

(a) 66.32% porosity, (b) 76.07% porosity.

4.2.5.2 EDAX

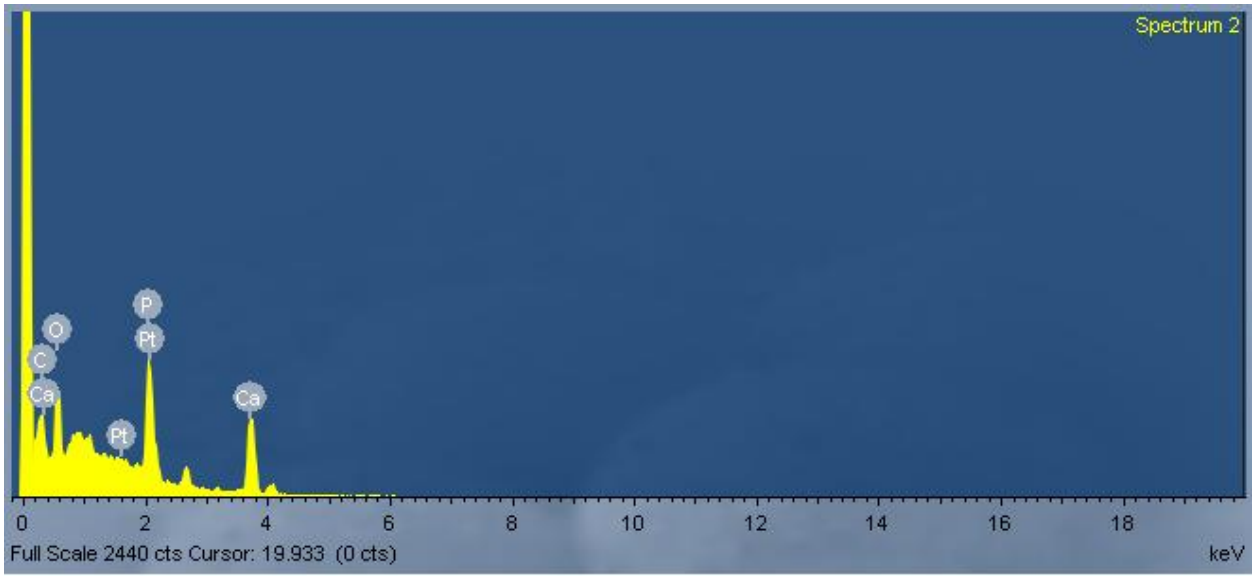

Fig. 4.11 Energy Dispersive X-ray Spectroscopy (EDAX) analysis of 76% porosity Hap Scaffold.

Energy dispersive X-ray spectroscopy (EDS or EDX) was another analytical technique which was used for the elemental analysis or chemical characterization of the SBF treated scaffold samples.

The above figure (Fig. 4.11) showed the **presence of calcium, oxygen, phosphorous** peaks only depicting the scaffold to be composed of these materials only. **Carbon** shown overlapping a calcium peak was present because of the in-vitro treatment of the scaffolds with SBF for a long time. Platinum shown overlapping a phosphorous peak was the result of Pt coating which was given for secondary electron imaging for SEM purposes. This elemental analysis confirmed the formation of carbonated Hap on the porous scaffolds, which indicated the bioactivity of the porous scaffolds.

Accuracy of EDS spectrum could have been affected by many reasons. Windows in front of the detector could have absorbed low-energy X-rays (i.e. EDS detectors cannot detect elements with atomic number less than 5, that is H, He, Li and Be). Over-voltage settings in EDS alter the peak sizes – raising over-voltage on the SEM shifting the spectrum to the larger energies, making higher-energy peaks larger and lower-energy peaks smaller. Also many elements would have overlapping peaks.

5. CONCLUSIONS

Conclusions

- ✓ Phase pure Hap was prepared from $CaNO_3.4H_2O$ and $(NH_4)_2HPO_4$ by co-precipitation method. Hap crystallized at a temperature of 1250^0C without the appearance of β-TCP phase.
- ✓ The porous scaffolds were prepared by using pore former PEG-600.
- ✓ Porous Hap scaffolds prepared from this method had porosities of 9.80%, 20.67%, 48.16%, 54.73%, 66.32%, 76.07%.
- ✓ The scaffolds had pore diameters in the range of ~100-400 μm and the pores were inter-connected.
- ✓ With increase in PEG-600 weights from 0.48 – 2.40 gms per gram of calcined Hap, the bulk density decreased and the apparent porosity increased.
- ✓ Increase in porosity from 9.80% to 76.07% led to decrease in compressive strength value from 8.873 Mpa to 0.179 Mpa.
- ✓ The pore size and pore inter connectivity depended upon the amount of pore former used.
- ✓ The peak volumes of Hg. intruded were achieved at lower pore diameters as the porosity increased to higher values as seen in the porosimetry graphs.
- ✓ In-vitro studies of bioactivity showed that the rate of tissue growth takes place rapidly in those scaffolds which had higher porosities (48.16%, 54.73%, 66.32% and 76.07% porosity samples).
- ✓ Carbonated Hap was deposited on the porous scaffolds, which indicated the bioactivity of the scaffolds studied here in this project.

6. REFERENCES

References

[1] LeGeros RZ, *Properties of osteoconductive biomaterials: calcium phosphates.* **Clin Orthop Relat Res** (2002) ;395:81–98.

[2] Akao M, Aoki H, Kato K. *Mechanical properties of sintered hydroxyapatite for prosthetic applications*. **J Mater Sci (**1981) ;16(3): 809–12.

[3] Yoshikawa T, Ohgushi H, Nakajima H, Yamada E, Ichijima K, Tamai S, et al. *In vivo osteogenic durability of cultured bone in porous ceramics: a novel method for autogenous bone graft substitution.* **Transplantation** (2000) ;69(1):128–34.

[4] De With G, Van Dijk HJA, Hattu N, Prijs K. *Preparation, microstructure and mechanical properties of dense polycrystalline hydroxy apatite*. **J Mater Sci** (1981) ;16(6):1592–8.

[5] Braddock M, Houston P, Campbell C, Ashcroft P. *Born again bone: tissue engineering for bone repair.* **News Physiol Sci** (2001) ;16:208–13.

[6] Goldberg VM, Stevenson S. *Natural history of autografts and allografts*. **Clin Orthop** (1987);225:7–16.

[7] Costantino PD, Friedman CD. *Synthetic bone graft substitutes*. **Otolaryngol Clin North Am** (1994) ;27:1037–74.

[8] Bonfiglio M, Jeter WS. *Immunological responses to bone.* **Clin Orthop** (1972) ;87:19–27.

[9] Langer R, Vacanti J.P., *Tissue Eng.*, **Science** (1993) ;260: 920–926.

[10] Ma P.X., *Scaffolds for tissue fabrication*, **Mater. Today**, (2004) ; 7(5) : 30–40.

[11] Hutmacher D.W., Schantz T, Zien I, Ng K.W., Teoh K.H., Tan K.C., *Mechanical properties and cell cultural response of polycaprolactone scaffolds designed and fabricated via fused deposition modelling*, **J. Biomed. Mater. Res.** (2001) ; 55 :203–216.

[12] V. Karageorgiou, D. Kaplan, *Porosity of 3D biomaterial scaffolds and osteogenesis*, **Biomaterials** 26 (2005) ; 27 : 5474–5491.

[13] Hulbert S.F., Young R.A., Mathews, Klawitter R.S., Talbert C.D., Stelling F.H, *Potential ceramic*

materials as permanently implantable skeletal prostheses, **J. Biomed. Mater. Res.** (1970) ; 4(3) : 433–456.

[14] Itali A.I., Ylanen H.O., Ekholm C, Karlsson K.H., Aro H.T., *Pore diameter of more than 100 microns is not requisite for bone in growth in rabbits*, **J. Biomed. Mater. Res.** (2001) ; 58(6) : 679–683.

[15] Leony Leon C.A., *New perspectives in mercury porosimetry.* **Adv Colloid Interface Sci** (1998) ;76 - 77:341–72.

[16] Livage J, Henry M, Sanchez C, **Prog. Solid State Chem**. (1988) ; 18(4) :259.

[17] Furth M.E., Atala A, Van Dyke M.E., *Smart biomaterials design for tissue engineering and regenerative medicine,* **Biomaterials**, (2007) ; 28: 5068-73.

[18] Ahoki H, *Medical applications for hydroxyapatite*, **St. Louis: Ishikayu Euro America Inc., Tokyo**, 1994.

[19] Eliott J.C., *Structure and chemistry of the apatites and other calcium-orthophosphates*. **Studios in Inorganic Chemistry 18, Elsevier, Amsterdam**, 1994.

[20] Vallet-Regí M, Arcos D, *Biomimetic Nanoceramics in Clinical Use*, **RSC. Nanoscience and Nanotechnology, Cambridge**, 2008.

[21] Stein H, D'Ambrosia R, Wolff's Law Decoded, http://www.orthosupersite.com/view.aspx?rid=26900.

[22] Mann S, Webb J, Williams R.J.P., *Biomineralization.*: *Chemical and Biochemical Perspectives*. **(Eds.), VCH**, USA, 1989.

[23] Cabañas M.V, Peña J, Román J, Vallet-Regí M, **J. Biomed. Mat. Res**. (2006); 78(A) : 508.

[24] Sánchez-Salcedo S, Nieto A, Vallet-Regí M, **Chem. Eng. J.** (2008); 137 :62.

[25] Hench L.L, Polar J.M, **Science**, (2002); 295 : 1014.

[26] Wise, Transtolo, Altobelli, Yaszemski, Gresser and Schwart., *Encyclopedic Handbook of Biomaterials and Bioengineering*, **Dekke, New York**, 1995.

[27] Sopyan I, Mel M, Ramesh S, Khalid K.A., *Porous hydroxyapatite for artificial bone*, **Science and Technology of Advanced Materials**, (2007); 8: 116–123.

[28] Ramay H.R., Zhang M, *Hydroxyapatite synthesis by sol-gel route*, **Biomaterials**, (2003); 24 : 3293.

[29] Potoczek M *"Hydroxyapatite foams produced by gelcasting using agarose"* **Materials Letters**, (2008); 62: 1055–1057.

[30] K.Schwartzwalder and A. V. Sommers, **US patent No. 3090094**, may 21 (1963).

[31] Thijs, I., Luyten, J. and Mullens, S, *Producing ceramic foams with hollow spheres*. **J. Am. Ceram. Soc.**, (2003), 87(1), 170–172.

[32] Itatani K, Uchino T, Okada I, *Preparation of Porous Hydroxyapatite Ceramics from Hollow Spherical Agglomerates Using a Foaming Agent of H2O2*, **Biomaterials** (2003), 34-39.

[33] Kwon S.H., Jun Y.K., Hong S.H. , Lee I.S., Kim H.E.; *"Calcium phosphate bioceramics with various porosities and dissolution rate"* , **J. Am. Ceram. Soc**, (2002), 85[12], 3129-31.

[34] Guo H , Su J, Wei J, Kong H , Liu C; *"Biocompatibility and osteogenicity of degradable Ca-deficient hydroxyapatite scaffolds from calcium phosphate cement for bone tissue engineering"* , **Acta Biomaterialia**, (2009); 5, 268–278.

[35] Deville, Saizaa and Tomsia, *Freeze casting of porous hydroxyapatite scaffolds for bone tissue engineering*, **J. Am. Cer, Soc**, 2006, 8, 112-115.

[36] Huang X, Miao X; *"Novel Porous Hydroxyapatite Prepared by Combining H2O2 Foaming with PU Sponge and Modified with PLGA and Bioactive Glass"*, **Journal of Biomaterial Application**, Volume 00 — 2006.

[37] Langer R, Cima L.G., Tamada J.A., Wintermantel E, *"Future directions in biomaterials"*, **Biomaterials**, (1990), 11; 738-745.

[38] Tas A.C., *"Synthesis of biomimetic Ca-hydroxyapatite powders at 370C in synthetic body fluids"* , **Biomaterials**, (2000); 21 : 1429-1438.